Fermilab

CDF/PUB/JET/PUBLIC/5792
FERMILAB-Conf-01/375-E December 2001

Recent QCD Results from CDF

Igor V. Gorelov *
(For the CDF Collaboration)
Dept. of Phys. and Astr., Univ. of New Mexico

Abstract

Experimental results on QCD measurements obtained in recent analyses and based on data collected with CDF Detector from the Run 1b Tevatron running cycle are presented. The scope of the talk includes major QCD topics: a measurement of the strong coupling constant α_s, extracted from inclusive jet spectra and the underlying event energy contribution to a jet cone. Another experimental object of QCD interest, prompt photon production, is also discussed and the updated measurements by CDF of the inclusive photon cross section at 630 GeV and 1800 GeV, and the comparison with NLO QCD predictions is presented.

1 Introduction

Although the topics of the talk outlined in the abstract concern different experimental objects, hadron jets and electromagnetic clusters in photon studies, they probe the common subtleties of perturbative QCD (pQCD) – NLO processes and non-perturbative contributions. Moreover the measurements include similar theoretical uncertainties such as renormalization μ_R and factorization μ_F scales and choice of PDF. From the experimental point of view,a hadron jet is a cone of radius R in η, ϕ over a seed *filled* with energy deposits contrary to a prompt photon object where the similar cone over el.-mag. cluster is required to be *"empty" to isolate* the cluster seed. The topic of underlying events covers specifically the study of the largest experimental (though inevitably connected with the theory) uncertainty in the jet inclusive measurement of α_s.

*the talk given on behalf of the CDF Collaboration at IX International Conference on Hadron Spectroscopy, August 25 - September 1, 2001, IHEP (Protvino), Russia.

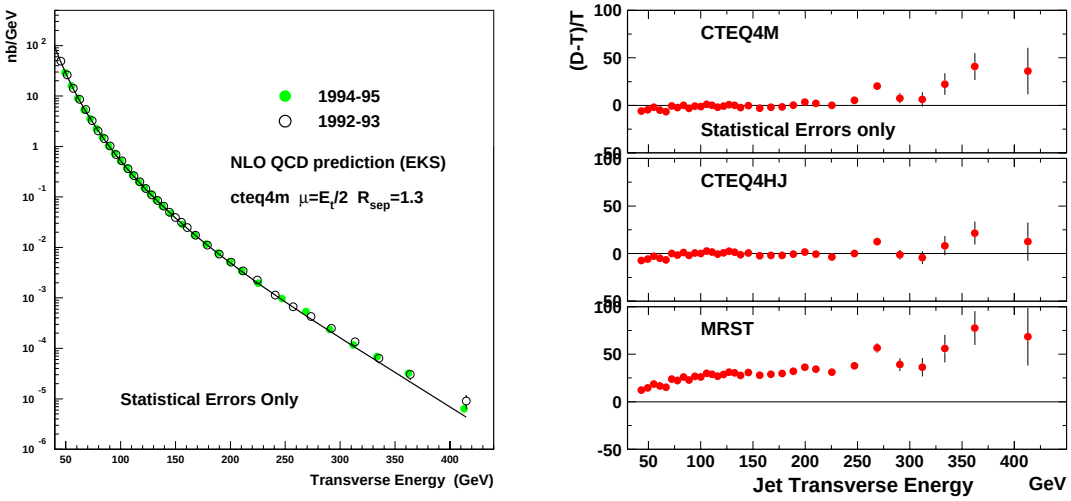

Figure 1: The corrected inclusive jet cross section (left) and the comparison to theory for various PDFs (right). Scales $\mu_R = \mu_F$ are set to $E_T^{jet}/2$ and phenomenological $\mathcal{R}_{sep} = 1.3$.

2 Measurement of the strong coupling constant α_s

The measurement of α_s is extracted from the inclusive jet differential cross section over the jet transverse energy E_T range from 40 GeV to 450 GeV. The measurements are based on a data sample of integrated luminosity $\mathcal{L} = 87pb^{-1}$ collected by CDF during 1994-95 (Run 1b) at $\sqrt{s} = 1.8TeV$. The CDF detector is described elsewhere [1]. The details of the inclusive jet cross section measurement can be found in [2]. Briefly, the iterative fixed cone algorithm with $R \equiv \sqrt{\delta_\phi^2 + \delta_\eta^2} = 0.7, \eta \equiv -\ln(\tan(\theta/2))$ is used. Only the central range of $0.1 < |\eta| < 0.7$ is considered. The raw experimental E_T spectrum is corrected bin by bin for the calorimeter response and resolution, for the underlying event energy using an iterative unsmearing procedure. The α_s is determined by comparing the jet cross-section with NLO pQCD, $\mathcal{O}(\alpha_s^3)$, calculations realized in the JETRAD Monte-Carlo program with NLO pQCD contributions incorporated [3]. To match the experimental efficiency of identifying overlapping jets, two partons are required to be separated by more than $\mathcal{R}_{sep} \times R$ with a phenomenological factor $\mathcal{R}_{sep} = 1.3$; otherwise they are merged into a single jet. The corrected inclusive jet cross sections for Run 1b and published Run 1a data are shown in the left picture of Fig. 1 with the scale parameters in JETRAD set as $\mu_R = \mu_F = E_T^{jet}/2$. The right plot shows that the choice of PDF can *accommodate* the discrepancy between theory and data. The statistical precision of data is significantly better than the systematics in measurement and theory. The Run 1b measurement is in impressive agreement with NLO pQCD predictions provided the flexibility allowed by current knowledge of PDFs. This agreement has led to the proposal to use inclusive jet data to determine α_s.

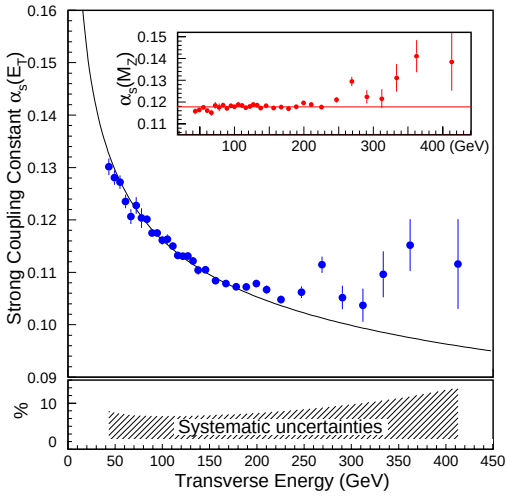

Figure 2: The running $\alpha_s(\mu_R = E_T^{jet})$ measurements. The inset plot shows the distribution of already evolved $\alpha_s(M_Z)$. The solid curve corresponds to an NLO pQCD prediction for the evolution $\alpha_s(E_T^{jet})$ using the averaged over (40...250)GeV bins value of $\alpha_s(M_Z) = 0.1178$.

Knowing that in the region $E_T^{jet} \in (40...450)GeV$ and $0.1 < |\eta| < 0.7$, the non-perturbative contributions are estimated to be negligible the NLO pQCD inclusive jet cross section can be parameterized as

$$d\sigma/dE_T = \alpha_s^2(\mu_R)\hat{X}^{(0)}(\mu_F, E_T)[1 + \alpha_s(\mu_R)k_1(\mu_R, \mu_F, E_T)]$$

Here both $\hat{X}(0)(...)$ and $k_1(...)$ are calculated by the JETRAD Monte-Carlo with NLO pQCD included. In this procedure the scale factors $\mu_R = \mu_F$ are set to E_T^{jet} unlike in comparisons of the inclusive jet cross section (see Fig. 1). The choice of PDF is CTEQ4M (see also below a discussion of theoretical systematics). Applying the same cuts and algorithms at the final parton level as are used in the data (JETRAD generator calculates weights) α_s is calculated for each of the 33 bins of the experimentally corrected $d\sigma/dE_T$ spectrum. These bin by bin calculations yield measurements of the *running* α_s presented in Fig. 2. The running $\alpha_s(\mu_R = E_T^{jet})$ for every point is evolved to the mass of Z^0, $\alpha_s(\mu_R = M_Z)$, using the evolution equation (inset plot in Fig. 2). Averaging over $E_T^{jet} \in (40...250)GeV$ yields:

$$\alpha_s(M_Z) = 0.1178 \pm 0.0001(stat.)$$

The points above 250 GeV increase the average by 0.0001.
As for the inclusive production measurement for bins below 250 GeV, there is good agreement with QCD while at higher E_T^{jet} the discrepancy has the same source as for the excess at the inclusive spectra (see left plot in Fig. 1). It is still not well understood but can be

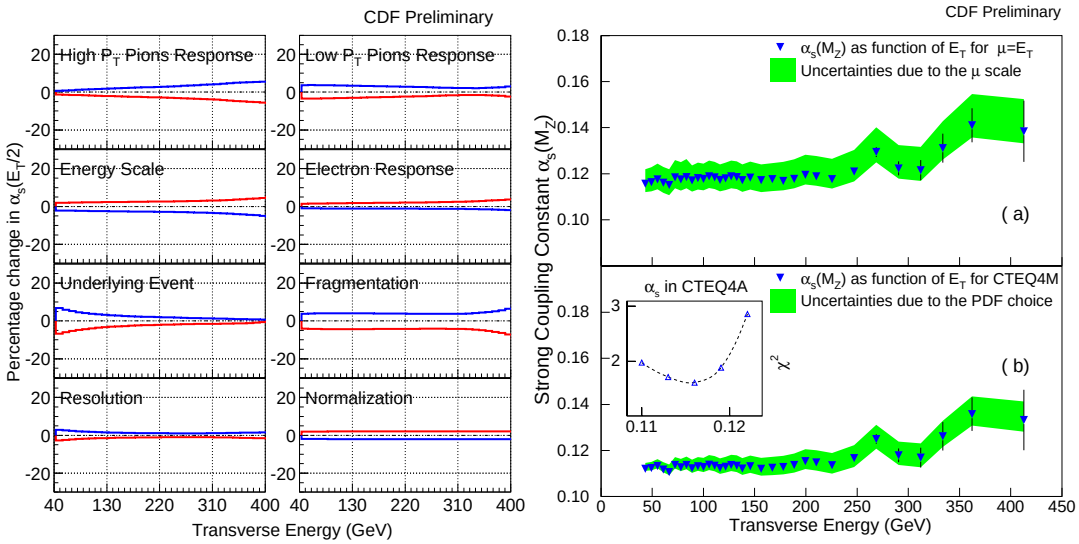

Figure 3: Experimental (left) and theoretical (right) systematic uncertainties in α_s.

adjusted with the appropriate choice of PDF and its high-x gluon component. To test the behavior of the evolved $\alpha_s(M_Z)$ with an energy E_T below 250 GeV, all 33 measurements have been fit with the linear function $P_0 + P_1 \times (E_T/E_T^0 - 1)$ with E_T^0 set to 92.8GeV. With $\chi^2/N_{d.o.f.} = 1.3$ the fit yielding $P_0 = 0.1176 \pm 0.0003, P_1 = 0.0003 \pm 0.0003$ proves an independence of $\alpha_s(M_Z)$ from E_T; that is pQCD predictions for the evolution of $\alpha_s(\mu_R)$ are *correct.*

Experimental systematic uncertainties (see breakdown of sources on left plots at Fig. 3) are derived from those on the inclusive jet cross section measurement. The dominant source is the calorimeter response to jets. In total the uncertainties propagated to $\alpha_s(M_Z)$ and summed in quadrature yield a total systematic experimental uncertainty of $\pm^{0.0081}_{0.0095}$.

Theoretical systematics includes (see left plots in Fig. 3) the uncertainty of renormalization scales μ_R, μ_F varied independently and reaching largest changes at $\mu_R = \mu_F$. The shift in $\alpha_s(M_Z)$ induced by variation is found to be $\pm^6_4\%$. Examining α_s^{PDF} for other PDF sets including CTEQ4A and MRST yields another uncertainty due to PDF choice to be $\pm 5\%$. The best agreement between data and theory over (40...250)GeV is found for CTEQ4M at $\alpha_s^{PDF} = 0.116$ *used in final fit.* Variation on $\mathcal{R}_{sep} = 1.3...2.0$ results in 5-7% changes in the cross section and induces a 2-3% uncertainty in $\alpha_s(M_Z)$.

Finally in conclusion of this topic the analysis results in a number obtained at $\mu_R = \mu_F = E_T$ as

$$\alpha_s(M_Z) = 0.1178 \pm 0.0001(stat.)^{+0.0081}_{-0.0095}(exp.syst.)$$

The theoretical uncertainties from PDF and μ-scale choices of $(\sim 5\% \oplus \pm^6_4\%)$ are *comparable* with the experimental systematics. The value is in *good agreement* with the world average $\alpha_s(M_Z) = 0.1181 \pm 0.0020$[5].

3 Underlying Event Energy Flow

The underlying event is the energy originating from soft spectator parton interactions while the hard partons produce jets. It appears as the energy deposited in a detector by particles from the breakup of interacting hadron beams, from initial state radiations in $2 \to 2$ and also due to semi-hard processes between spectators like multiple parton scattering. It is an essentially non-perturbative contribution.
As the jet clustering is based on a fixed cone algorithm, there is a contribution due to the underlying event energy flowing into that cone. This energy needs to be subtracted.
The similarity with minimum bias events is used presently as an assumption for energy corrections. Unfortunately the large uncertainty $\sim 30\%$ on the contribution to the energy scale induces the largest uncertainty ($\sim$ 15...20% at low energy range) in the inclusive jet cross section analysis. Therefore adequate estimates of underlying event energy are of *vital importance*.
In the analysis the jets in a jet event sample are reconstructed with a jet cone radius $R = 0.7$ in the central $|\eta| < 0.7$ region while in a minimum bias data sample a *random* η of a "lead jet" is taken with the same definitions. For each event two cones w.r.t. the leading jet at $\eta = \eta_{LeadJet}$ and having $\phi = \phi_{LeadJet} \pm 90^\circ$ are inspected. These two cones at 90° are presumed to be in a semi-quiet region, far away from the two leading jets, though still in central rapidity region. Considering energy E_T flowing into 90° cones, the cones are sorted by energy and identified as "Max. cone" and "Min. cone". The Max. cone most probably will contain NLO corrections to $2 \to 2$ while the most quiet Min. cone gives an indication of the amount of the underlying event. The difference between energies contained in Max. and Min. cones is taken as an indication of NLO contributions. The behavior of E_T energy flow in every cone and their difference versus E_T of the leading jet is shown in Fig. 4 (left and right plots correspondingly) for data taken at $\sqrt{s} = 1800 GeV$. First of all *the flatness* of the E_T energy flowing into the Min. cone versus $E_T^{LeadJet}$ is remarkable while E_T in the Max. cone increases with $E_T^{LeadJet}$. The similarity in shape of the distributions is reproduced in the CDF detector simulated (QFL program) Herwig Monte-Carlo data sample. There is an evident offset between data and Monte-Carlo of $\sim$800MeV for Max. cone and $\sim$500MeV for Min. cone.
For the min. bias data sample (see the same Fig. 4) we consider a *random cone* at $\eta_{\text{"}LeadJet\text{"}}$ in the same central $|\eta| < 0.7$ region and examine the $E_T^{\text{"}LeadJet\text{"}}$ in that cone to be the level of E_T energy flow. The Min. cone E_T for the jet data sample is higher than the level of E_T in a *random cone* for min. bias events by $\sim$300MeV. The behavior is similar for corresponding Monte-Carlo samples.
The above considerations give a clear indication that underlying events of jet data include an "echo" from the hard interaction and are not adequate to min. bias ambient energy flow and that Herwig model for min. bias does not give a unified description for soft and hard physics.
One has to mention that both in jet and min. bias data there is *an offset* of $\sim$500MeV and $\sim$680MeV between *data and Monte-Carlo* simulation.

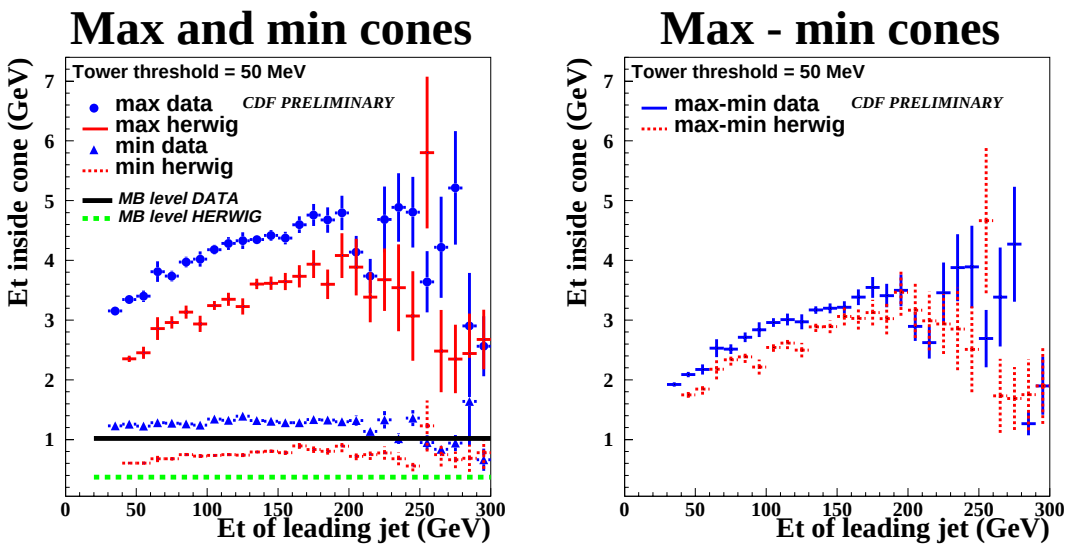

Figure 4: The energy flow into Max. and Min. cones (left) and the difference between energy flow into max. and min. cones (right).

It is interesting to have a look at the difference of energies

$$E_T^{Max.cone} - E_T^{Min.cone}$$

– this can be taken as an estimate of the "NLO correction" to $2 \to 2$ (see a right plot at Fig. 4). Here the underlying event energy expected to be minimized and data agree with Monte-Carlo in shapes having still an offset of ∼300MeV. The distribution drops at very high E_T due to poor statistics.
The alternative to "Min., Max. cones" and their subtraction approach is a calculation of total transverse energy:

$$E_T^{SwissCheese} = \sum_{towers}^{|\eta|<0.7} E_T^{tower} - \sum_{jet=1}^{2\ or\ 3} [\sum_{towers}^{jet} E_T^{tower}]$$

Here we require $E_T^{Jet} > 5GeV$ – see Fig. 5. In the left plot of Fig. 5 the 2 jet subtracted energy should contain mainly NLO (3rd parton) but the 3 jet subtracted energy should have little of NLO; but data and "Herwig + CDF simulation" points are still higher (with a slope) than min. bias data level. This difference indicates possible contributions from hadronization of jets, multiple (double) parton scattering and higher order radiations.
To understand data and Monte-Carlo difference *an independent analysis based on tracks* has been undertaken (see also [6]). Similar quantities have been constructed using tracks instead of calorimeter towers – see the right plot of Fig. 5. The plot shows a total track P_T flow inside Max. and Min. cones again versus calorimeter $E_T^{LeadJet}$ at $\sqrt{s} = 1800GeV$ with data–Monte-Carlo difference disappearing. The agreement is also good for other

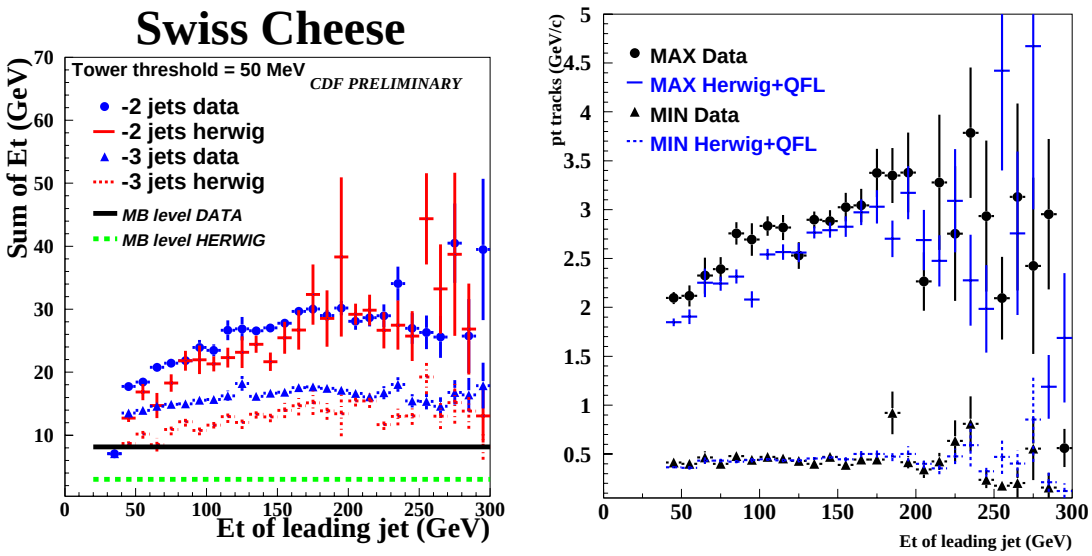

Figure 5: Total transverse energy with jets excluded (left plot) and total track P_T flow inside Max. and Min. cones (right plot), track analog of calorimeter E_T flow

.

plots where tracks substitute towers in Max. and Min. cones at 90°. Again here the min. bias data level is $\sim 20\%$ smaller than the min. cone jet data level. As we have already observed with calorimeter towers, the min. bias spectra are "softer" than the underlying event spectra from the jet data sample.
Also from track based plots we conclude that the reason for the discrepancy in "calorimeter vs. tracks" lies in the scale at low energies.
In a summary of the "Min., Max. cone" analysis one should mention several points:

- Using "Min., Max. cone" approach we found that energy in Min. cone forms a plateau against energy of a leading jet and exhibits the behavior of underlying events. The height of this plateau is larger than the one observed in min. bias data.
- The total E_T energy with 3 jets contribution subtracted also exhibits the flattening in data and Herwig + "CDF simulation".
- Disagreement in energy flow (Min. cone, "Swiss Cheese") for jet samples with min. bias events indicates the presence of semi-hard multiple hadron interactions and other higher order effects in underlying events which are not present in min. bias samples. Consequently the Herwig model for min. bias events does not give a unified description for soft and hard physics.
- We find the offsets between our data and "Herwig + CDF simulation" at calorimeter level.

- The reason for the offset of data relative to "Herwig + CDF simulation" is still under investigation but may probably be due to the under-estimation of low energy deposits in the calorimeter.
- The Monte-Carlo models should be tuned to better describe the underlying event in $p\bar{p}$ collisions.

4 Isolated Prompt Photon Cross Sections

Here we discuss another object of QCD interest – prompt photon production in hadronic interactions at Tevatron. The prompt (or direct) photons involve both LO and NLO pQCD processes briefly listed below:

- $gq \to q\gamma$ – *dominating diagram*
- $q\bar{q} \to g\gamma$ – LO annihilation
- $q\bar{q} \to g\gamma g, qg\gamma$ – NLO initial and final state rad. corrections
- photon bremsstrahlung – produced along with hadrons, *suppressed* by photon isolation cuts (see below)

The prompt photon is identified as *an isolated* electromagnetic object, not accompanied by *nearby* energy flow coming from neutral component of hadron jets like π^0, η.
The analysis exploits the electromagnetic clusters from the electromagnetic compartment of CDF central calorimetry (CEM), with lateral profile measured in the proportional chamber CES positioned in the CEM at a depth of shower maximum and the fraction of events with conversions in $1.075X_0$ of magnet coil counted by proportional chamber CPR installed just in front of the CEM.
The data used in the analysis were taken during 1994-95 (Run 1b). The trigger requires cluster energy $E^{elm}_{cluster} > Thr$ with three thresholds: Thr = 10, 23, 50 GeV corresponding to three event samples. The important cuts and selection criteria are

- *isolation* criteria – require energy deposited in a cone of $R \equiv \sqrt{\delta^2_\phi + \delta^2_\eta} = 0.4$ around $E^{elm}_{cluster}$ to be $E^{elm}_{isol.cone} < 1GeV$
- consider only central region $|\eta|$ <0.9
- $|Z_{vertex}|$ <60cm
- require *NO* charged reconstructed track pointing to CPR
- require *NO* other photon above 1GeV in CES to suppress further multiple π^0, η

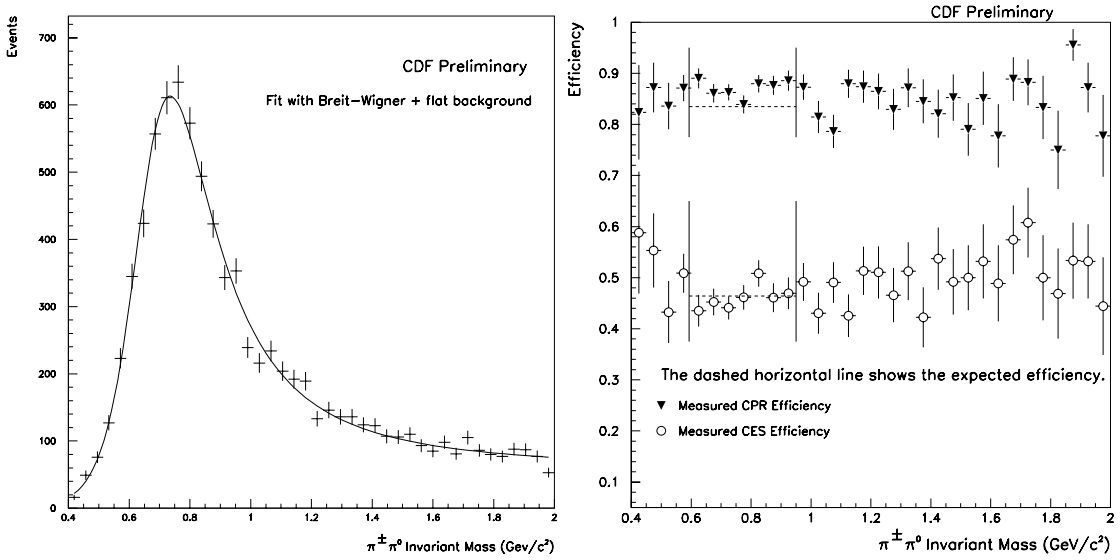

Figure 6: $\mathcal{M}(\rho^{\pm} \to \pi^0\pi^{\pm})$ mass spectrum (left histogram) and background efficiency (right plot). The signal band is $\mathcal{M}(\rho^{\pm}) \in (0.6, 0.95) GeV/c^2$ and the background band – $\mathcal{M}(\rho^{\pm}) \in (1.7, 2.0) GeV/c^2$.

The signal efficiency of these cuts for *prompt photons* is $\sim 39\%$. The main remaining backgrounds are single π^0, η . This neutral el.-mag. background is subtracted statistically applying two methods – the profile method and the conversion method (see [7] for details). For both methods one determines in every P_T bin the number of signal events as

$$N_{1\gamma} = \left(\frac{\epsilon_{data} - \epsilon_{bgr}}{\epsilon_{1\gamma} - \epsilon_{bgr}} \right) N_{data}$$

The profile method is based on parameterized shower profile in CES chambers measured in electron test beam. Then the profile (broader for multiphoton background) is fit to test beam data on an event by event basis. The signal and background efficiencies are determined from CDF Monte-Carlo simulation. This method is good for low energy photons with P_T <36 GeV/c.
The conversion method is based on counting with the CPR the photon conversions in the solenoidal coil and used for prompt photons with P_T >36 GeV/c. The background of multiple photons convert more readily than a single prompt photon signal. The signal efficiency of $\epsilon_{1\gamma} \sim 1 - \exp(-7X_0/9) \approx 60\%$ and the background efficiency of $\epsilon_{bgr} \sim 1 - (1 - P_{1\gamma})^2 \approx 84\%$ are applied as *weighting factors* for the data on an event by event basis. For both methods ϵ_{bgr} is measured using the reference data sample of π^0 produced from decay $\rho^{\pm} \to \pi^{\pm}\pi^0, \pi^0 \to \gamma\gamma$ (see Fig. 6). For the conversion method, the weighting function ϵ_{bgr} has been *recalibrated* using the experimental $\rho^{\pm}$ data sample. One has to mention that for the profile method based on $\rho^{\pm}$ data $\epsilon_{bgr} = 46.1 \pm 1.0\%$ to be compared with expected $\epsilon_{bgr} = 46.4 \pm 0.4\%$. For the conversion method based on $\rho^{\pm}$ data

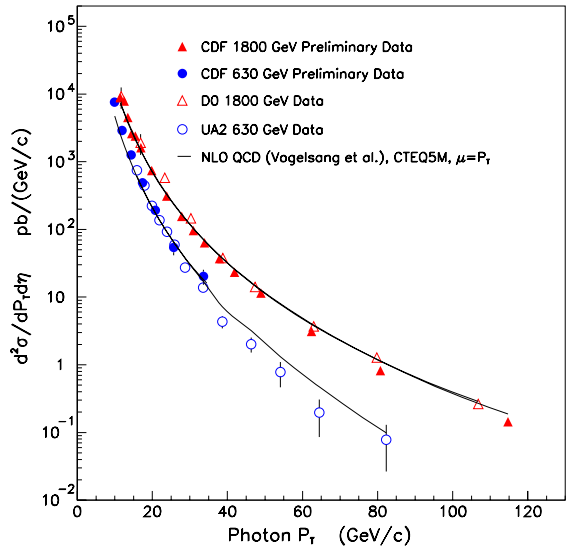

Figure 7: The prompt photon inclusive cross section at 1800 GeV and 630 GeV with D0 and UA2 results overlapped.

$\epsilon_{bgr} = 86.8 \pm 0.7\%$ while the expected (based on weighting function) $\epsilon_{bgr} = 83.2 \pm 0.7\%$. Here the weighting function has been recalibrated to match the data.
Finally we derive the prompt photon inclusive cross section in P_T bins shown in Fig. 7 (see also the recent CDF publication in [8]) CDF 1800 GeV and 630 GeV data agree well with the corresponding D0 and UA2 measurements. The comparison of data at $\sqrt{s} = 1800GeV$ with NLO pQCD calculations shown versus absolute P_T in the right plot of Fig. 8 uses the CTEQ4M PDF, includes NLO fragmentation terms, and uses considerably varied μ-scale choices – *NO* combination has been found that matches the shape of data to within several σ.
The left plot in Fig. 8, showing the difference between data and theory versus scaled momentum $X_T = 2P_T/\sqrt{s}$, exhibits a rise in the measured cross section below 0.1, indicating an enhanced soft gluon contribution which is spoiling the agreement with NLO. Again CDF data points are in agreement with corresponding D0 and UA2 points. But the CDF data points $(D-T)/T$ for $\sqrt{s} = 630GeV, 1800GeV$ are different by $\sim 50\%$ while the experimental uncertainties are of $\sim 9\%$ only. There is *disagreement* with theory predictions at the *low X_T region which is rich with gluon content.*
One possibility to correct standard NLO pQCD with typical settings to match the data is adding K_t as part of the non-collinear initial state radiation. Both plots in Fig. 9 demonstrate that this works well to describe the shape of the data for both energies. The other curve is a more fundamental attempt by Baer-Reno[9] to add a parton shower to NLO pQCD.
In conclusion of this topic, CDF has updated and improved prompt photon measurements at $\sqrt{s}$ =630GeV and 1800GeV. Data show at low X_T the effect of soft multiple gluon

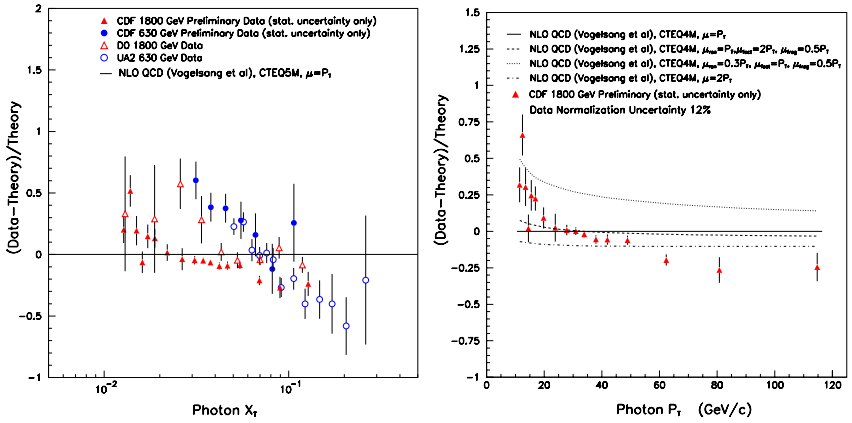

Figure 8: Data versus NLO pQCD predictions: X_T spectra (left plot) and P_T spectra (right plot).

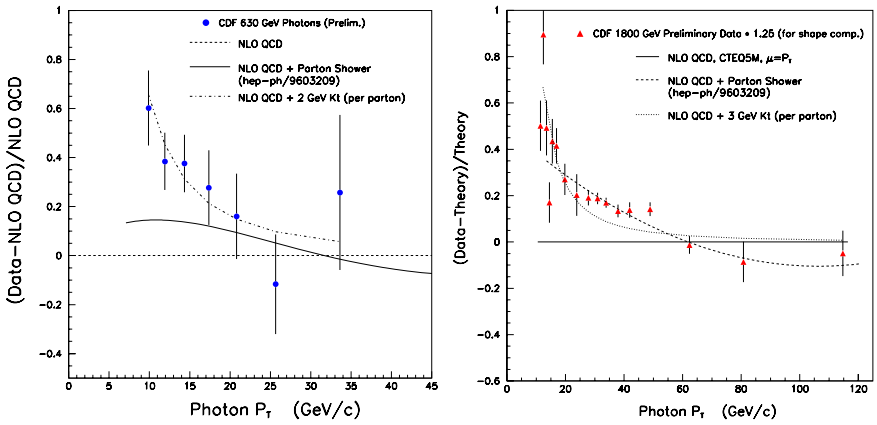

Figure 9: Data versus theory for 630 GeV (left) and 1800 GeV (right) with added K_t.

emission. Theory does not describe CDF data at both energies at low X_T. Prompt photon production continues to be a good place to test modern NLO pQCD calculations. *Ad hoc* inclusion of K_t smearing effects in simple Gaussian smearing models works well, though for gluon distribution studies one needs more fundamental approaches.

5 The Acknowledgments

The author is grateful to his colleagues from the CDF QCD working group for useful suggestions and comments made during preparation of this talk. The author would like to thank Prof. Sally C. Seidel for support of this work, fruitful discussions, and comments.

References

[1] F. Abe et al., The CDF Collaboration, *Nucl. Instrum. Methods*, **A271**, 387(1988).

[2] T. Affolder et al., The CDF Collaboration, *Phys. Rev.*, **D64**, 032001(2001).

[3] W. Giele, E.W.N. Glover and J. Yu, *Phys. Rev.*, **D53**, 120(1996).
W. Giele, E.W.N. Glover and D.A. Kosower, *Phys. Rev. Lett.*, **73**, 2019(1994).

[4] T. Affolder et al., The CDF Collaboration, FERMILAB-CONF-01/246-E. Submitted to *Phys. Rev. Lett.*, August 22, 2001.

[5] D.E. Groom et al., Particle Data Group, *Eur. Phys. J.*, **C15**, 1(2000).

[6] T. Affolder et al., The CDF Collaboration, Charged Jet Evolution and the Underlying Event in Proton-Antiproton Collisions at 1.8 TeV, FERMILAB-PUB-01/211-E. Submitted to *Phys. Rev.* **D**, November 24, 2001.

[7] F. Abe et al., The CDF Collaboration, *Phys. Rev. Lett.*, **68**, 2734(1992).
F. Abe et al., The CDF Collaboration, *Phys. Rev.*, **D48**, 2998(1993).
F. Abe et al., The CDF Collaboration, *Phys. Rev. Lett.*, **73**, 2662(1994).

[8] D. Partos and S. Kuhlmann, Comparison of the Direct Photon Cross Sections at $\sqrt{s}$=1.8 TeV and $\sqrt{s}$=0.63 GeV, CDF Note CDF/ANAL/JET/CDFR/5636, November 30, 2001. To be published in *Phys. Rev.* **D**.

[9] H. Baer and M.H. Reno, *Phys. Rev.*, **D54**, 2017(1996).